Phase Behavior of Methane Haze

R. Signorell* and M. Jetzki

Department of Chemistry, University of British Columbia, 2036 Main Mall, Vancouver, BC V6T 1Z1, Canada

(Received 27 August 2006; published 4 January 2007)

Methane aerosols play a fundamental role in the atmospheres of Neptune, Uranus, and Saturn's moon Titan as borne out by the recent Cassini-Huygens mission. Here we present the first study of the phase behavior of free methane aerosol particles combining collisional cooling with rapid-scan infrared spectroscopy *in situ*. We find fast (within minutes) phase transitions to crystalline states directly after particle formation and characteristic surface effects for nanometer-sized particles. From our results, we conclude that in atmospheric clouds solid methane particles are crystalline.

DOI: 10.1103/PhysRevLett.98.013401 PACS numbers: 36.40.Ei, 36.20.Ng, 96.12.Jt, 96.30.nd

Methane aerosols are among the main constituents in the atmospheres of the giant planets Neptune [1–3] and Uranus [3,4] and of Saturn's moon Titan [3,5–9]. Most recently, the Cassini-Huygens mission has established the role of methane in Titan's atmosphere [5–9] as a counterpart to terrestrial water [10–13] for cloud and rain formation. Icy methane particles critically influence the energy balance and the composition of these atmospheres, through phase transitions, mass transfer processes, and chemical and photochemical reactions. In spite of the ubiquitous occurrence of methane aerosols, however, their properties are still largely unexplored, as their laboratory investigation poses a significant experimental challenge [14–17]. In atmospheric clouds, methane ice particles exist as unsupported free particles, i.e., as aerosols. Bulk studies cannot provide reliable data here because they do not contain any information about the influence of intrinsic particle properties such as size, shape, surface structure, and phase. The only alternative is to study the properties of methane particles directly in the aerosol phase. This is particularly true for nanometer-sized molecular aggregates (1–10 nm) whose properties significantly deviate from those of the bulk, mainly because of the large fraction of surface molecules (up to 90%). Nanometer-sized methane ice particles play a uniquely important role. They not only occur as stable constituents of particle clouds, but they also act as essential intermediates both in the formation and in the degradation of all larger particles where their phase behavior may have an important influence.

The present contribution constitutes the first study ever of the phase behavior of free methane ice particles. It reports direct infrared spectroscopic observations of different phases and phase transitions in methane aerosols at temperatures between 6 and 80 K. Because of their absorption strengths, the triply degenerate stretching mode ν_3 at $\sim 3010\ \mathrm{cm}^{-1}$ and the triply degenerate bending mode ν_4 at $\sim 1300\ \mathrm{cm}^{-1}$ [18–20] are the most important midinfrared bands for remote sensing of methane ice. The ν_4 band is particularly interesting since it is well separated from the bands of other hydrocarbon solids. Under the conditions of our experiment, bulk methane exists in two different crystalline cubic phases [21–23]. The stable phase above a temperature of 20.4 K is called phase I; the stable phase below this value is referred to as phase II. In both cases, the carbon atoms at the center of tetrahedral methane molecules occupy a face-centered cubic lattice. In phase I, all tetrahedral molecules are orientationally disordered. Phase II is a partially orientationally ordered structure, which has two types of site symmetry D_{2d} and O_h. The space group is $Fm3c$ with eight molecules per primitive unit cell. Six of the eight CH_4 molecules are ordered and occupy the D_{2d} sites. The orientation-dependent octupole-octupole interaction leads to this partial order. The two other molecules in the unit cell occupy O_h sites and perform slightly hindered rotations [24,25]. The two different phases exhibit characteristic patterns in the infrared spectra of methane bulk [18–20]. The orientational disorder of phase I leads to broad unstructured midinfrared bands, while the partial order and rotational motion in phase II results in structured bands consisting of several individual absorptions [26].

Methane aerosol particles were generated by bath gas cooling in a specially designed collisional cooling cell [14–17]. Infrared extinction spectra were recorded *in situ* in the cold cell during the phase transition with a rapid-scan Fourier transform infrared spectrometer (time resolution 30 ms, spectral resolution $2\ \mathrm{cm}^{-1}$). Prior to particle generation, the precooled cell (6–80 K) was filled with He bath gas, which after some minutes thermally equilibrated with the cell. The particles were then formed by rapid injection of a CH_4/He gas mixture (800 ppm CH_4 in He) into the cold He bath gas. This rapid cooling led to supersaturation of the methane gas and, thus, to ice particle formation. Bath gas cooling is a unique method to study properties of ice particles. It allows the investigation of unsupported free particles in thermal equilibrium with the bath gas, which rendered it possible to measure phases and phase transitions in methane aerosol particles.

Figure 1 shows typical infrared spectra of methane aerosols in the region of the ν_3 fundamental on the left

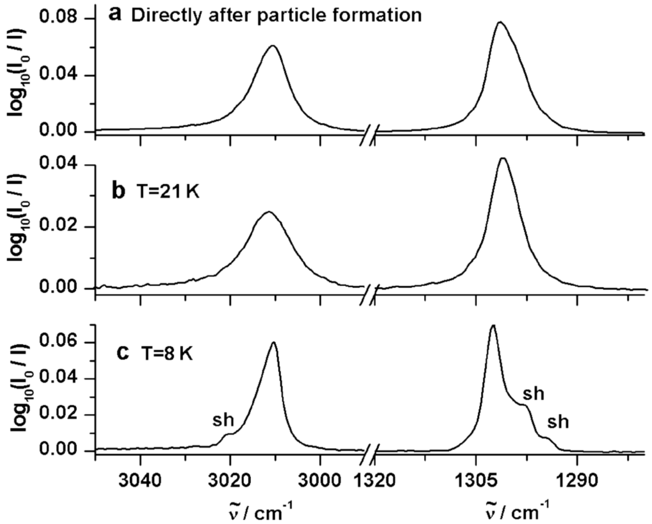

FIG. 1. Experimental infrared spectra of methane aerosols. (a) Amorphous phase directly after the particle formation. (b) Stable particle phase after the phase transition above 20.4 K. This phase corresponds to the crystalline bulk phase I [see Fig. 2(a)]. (c) Stable particle phase after the phase transition below 20.4 K. This phase is a combination of bulk phases I and II (see Fig. 3).

and in the region of the ν_4 fundamental on the right. The particle radius lies around 5 nm, and the particle number concentration has a value of about 10^9 particles per cm^3 aerosol. The dependence of particle size and abundance on the sample gas concentration was determined in a series of experiments for particle sizes up to several hundred nanometers. For sufficiently strong scattering, the particle size can be deduced directly by fitting the spectra using Mie theory. Smaller particle sizes were determined by extrapolating to lower sample gas concentration. The procedure used is very similar to that described in Ref. [14] and references therein. We have tested the reliability of these results for methane by comparing them with our previous findings for nanometer-sized ammonia aerosols for which we could determine the sizes independently from a band shape analysis using a microscopic model as described in Ref. [17]. The experimental conditions (bath gas pressure and sample gas concentration) were chosen so that no significant agglomeration and coagulation occurred during the time scale of the experiment. These conditions were determined from corresponding experiments with ammonia and CO_2 particles for which agglomeration and coagulation can be detected sensitively in the infrared spectra due to the strong shape-dependent exciton coupling [14,16,17]. Figure 1(a) depicts the spectrum measured directly after the particle formation. It shows unstructured broad, slightly asymmetric bands, which are characteristic of an amorphous state [19]. Directly after the particle formation, the same broad asymmetric band shapes were observed at all different bath gas temperatures. We thus conclude that below the melting point independently of the temperature the particles are initially formed as amorphous aggregates. Within about 5 min after the particle formation, temperature-dependent phase transitions take place in the cooling cell. They are monitored by continuous changes of characteristic spectral features. After that period, the spectra remain stable. At temperatures above 20.4 K, the spectra look like the one depicted for 21 K in trace (b), while at temperatures below 20.4 K they resemble the spectrum shown for 8 K in trace (c) in Fig. 1. At 21 K, the bands are still broad after the phase transition, but contrary to the amorphous phase [Fig. 1(a)] they now have a symmetric shape. At 8 K, the infrared bands are clearly structured with a main peak and several shoulders. Apart from these effects, we could not observe any dependence of the time evolution of the phase transition on experimental parameters within the present limits of their tuning ranges.

In analogy to the behavior of solid methane bulk, one would expect that after the phase transitions the ice particles are in phase I at a bath gas temperature above 20.4 K and in phase II below this value [21–23]. To verify this expectation, we compare our results for particles with bulk data. A direct comparison with bulk infrared spectra [18–20] is not meaningful, since particle spectra show different band positions and intensities compared with bulk spectra—a consequence of the finite particle size. A meaningful comparison with bulk data is possible only if experimental refractive index data of the solid bulk [27] in combination with classical scattering theory [28] are used to calculate particle spectra. These calculated particle spectra can then be compared directly with the experimental ones. We have already demonstrated in previous investigations (see [16] and references therein) that band positions and band intensities in particle spectra can significantly deviate from corresponding bulk spectra. We have also shown that these changes are reproduced at least qualitatively by scattering calculations even for compounds for which different sets of refractive index data exist. For CH_4, we have compared two different sets of refractive index data and found that our results are not sensitive to the set of refractive index data chosen. That the refractive index of the bulk is still valid for the particles is also confirmed by neutron scattering data of methane in mesopores (radii 6–18 nm) which show the same crystal structures as the bulk [29]. Figure 2 shows the calculated methane particle spectra at bath gas temperatures of 21 and 8 K. The band positions of the experimental and the calculated spectrum listed in Table I agree within the uncertainties, demonstrating that the particle size effect on band positions is almost perfectly reproduced by the calculations. For the 21 K spectrum, in addition to the band positions, also the overall agreement between the experimental [Fig. 1(b)] and the calculated [Fig. 2(a)] spectra is very good. Hence, we conclude that above 20.4 K the methane particles undergo a fast phase transition within minutes after their formation from an unstable amorphous

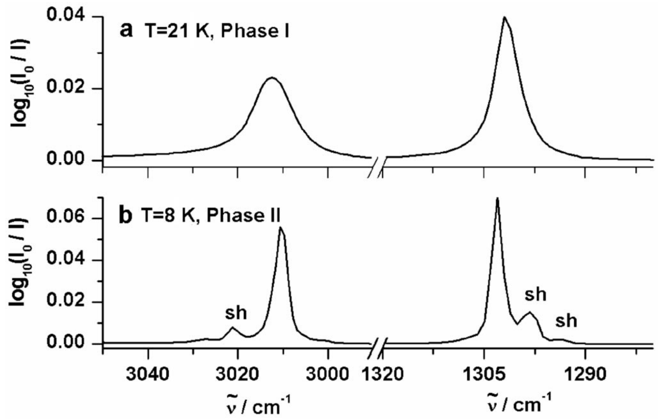

FIG. 2. Calculated infrared spectra of methane aerosols. (a) For particles with the structure of the cubic bulk phase I at 21 K. In this phase, the methane molecules are orientationally disordered. (b) For particles with the structure of cubic bulk phase II at 8 K. Some methane molecules are orientationally ordered in this phase.

state [Fig. 1(a)] to the stable crystalline cubic phase I [Figs. 1(b) and 2(a)]. The broad unstructured bands arise from orientational disorder of the tetrahedral molecules in phase I.

At 8 K, however, the overall agreement between experiment [Fig. 1(c)] and calculation [Fig. 2(b)] is clearly less satisfactory. Compared with the calculated spectrum, the experimental spectrum has additional contributions from unstructured broad components. These observations clearly show that this stable particle phase does not completely coincide with the crystalline bulk phase II. How can this deviation between particles and bulk phase II be understood? Particles in the lower nanometer range consist to a large extent of the surface region. If we assume that the surface region of the 5 nm methane particles has a thickness of about one unit cell (~ 1 nm [21]), already 50% of all methane molecules of a particle lie in this surface region. Because of the influence of the boundary, the intermolecular forces between different CH_4 molecules are altered in this surface region compared with the core region of the particles. In the surface, the symmetry is broken, and it is thus unlikely that the CH_4 molecules are partially ordered by octupole-octupole interaction as is the case in bulk phase II. It is much more plausible that all surface molecules remain orientally disordered similar to the high-temperature phase I. For the particle's core, however, nothing speaks against a partial orientational order as in bulk phase II. Consequently, we propose that methane particles below 20.4 K consist of a core region with the structure of bulk phase II and a surface region with the structure of bulk phase I.

Figure 3 compares the experimental spectrum at 8 K after the phase transition (trace *a*) with the calculated spectrum of a surface-core particle (trace *b*), i.e., phase I in the surface and phase II in the core. The agreement between the two spectra validates our assumption. As a result of the contribution of phase I in the surface, the calculation now reproduces the additional unstructured contribution observed in the experimental spectrum. This was not the case for the calculation assuming pure phase II particles [Fig. 2(b)]. Similar surface-core architectures were also found for solid methane in mesopores of controlled-pore glasses with pore radii between 6 and 18 nm using neutron scattering [29]. The core of these pores consists of methane in phase II which is covered by a thin methane layer at the pore walls without long range structure. The radius of this layer amounts to about 2 nm independently of the size of the pores. We have also found

TABLE I. Positions of infrared band maxima $\tilde{\nu}$ in wave numbers of main peaks and shoulders (sh) for CH_4 aerosol particles.

Temperature (K)	Type of band	Exp. in Fig. 1 $\tilde{\nu}/\mathrm{cm}^{-1}$	Calc. in Fig. 2 $\tilde{\nu}/\mathrm{cm}^{-1}$
21	ν_3	3011.5	3012
21	ν_4	1301.1	1302
8	ν_3(sh)	3020.9	3021
8	ν_3	3010.2	3010
8	ν_4	1302.5	1303
8	ν_4(sh)	1297.6	1298
8	ν_4(sh)	1294.5	1294

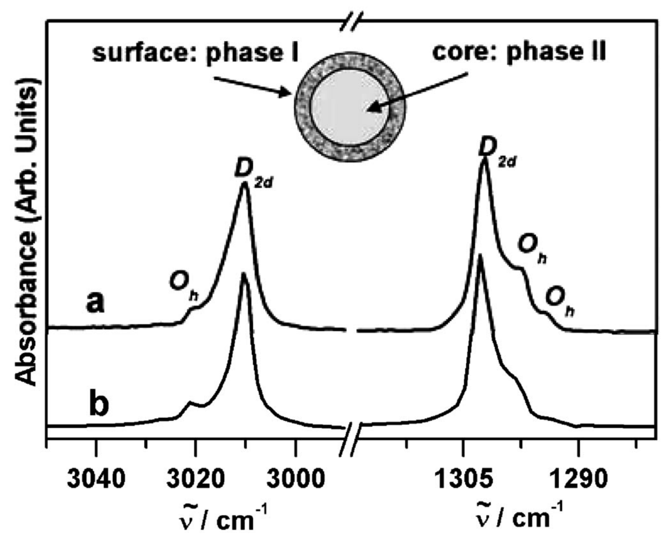

FIG. 3. Surface effects in nanometer-sized methane aerosol particles. (a) Experimental particle spectrum after the phase transition below 20.4 K in Fig. 1(c). (b) Calculated particle spectrum for a 5-nm particle with a surface-core structure consisting of two different phases. The surface (dimension 1 nm) consists of bulk phase I, and the core (4 nm) consists of bulk phase II. The structure in the spectra arises from bulk phase II in the core. The main peaks are caused by D_{2d} molecules, and the shoulders correspond to the rotational structure of O_h molecules. Bulk phase I in the surface leads to unstructured broad contributions.

a similar surface-core structure with a crystalline core and a less structured surface for nanometer-sized ammonia particles with different sizes below 10 nm [17]. The analysis with a microscopic model also led to a surface region size of 1–2 nm for all particle sizes. We think that these two results strongly support our interpretation given here. From the comparison of calculations with experimental data, we find that the thickness of the surface of our methane aerosol particles discussed here most likely lies between 0.5 and 1.5 nm. The same arguments as given for ammonia particles in Ref. [17] also hold here to exclude the formation of surface-core particles with a less structured core and a crystalline surface as well as the formation of a mixture of particles having different phases. The particle formation process speaks against the first type of particles [17]. The fact that we could not observe any temperature or pressure dependence (below 20.4 K) of the crystallization process and the fact the crystallization process is complete after 5 min speak against the formation of particles having different phases. We performed our calculations with one single mean particle size since we cannot obtain a size distribution from our spectra. We have tested, however, that the result is not altered when a typical size distribution found for aerosols in cooling cells [16] is used instead. As a result, we conclude that below 20.4 K the particles undergo a fast phase transition from an unstable amorphous phase to a stable crystalline state with a surface-core architecture.

The special phase behavior of methane haze may significantly influence the evolution of clouds in the atmospheres of Neptune [1–3], Uranus [3,4], and Titan [3,5–9]. Fast phase transitions (within minutes) to crystalline states observed at all temperatures below the melting point suggest that, under the atmospheric conditions of Neptune, Uranus, and Titan, solid methane particles are mainly present in the crystalline phase I. For example, through vapor pressure effects this finding influences particle sizes in the clouds and thus particle sedimentation velocities and the heat balance in the clouds [3,7,11]. Surface effects in nanometer-sized particles [13,17] play a special role in this context, since these particles are always involved in the formation and degradation of larger particles. The fact that methane haze particles are crystalline below the melting point may also affect chemical processes, since heterogeneous reactions and photochemical processes depend on the phase. Similar phase effects are expected to play a crucial role in water ice clouds of the Earth's atmosphere [10–12].

We are grateful to the Natural Sciences and Engineering Research Council of Canada and the Deutsche Forschungsgemeinschaft for financial support.

*Electronic address: signorell@chem.ubc.ca

[1] B. A. Smith *et al.*, Science **246**, 1422 (1989).
[2] S. G. Gibbard *et al.*, Icarus **166**, 359 (2003).
[3] A. Sánchez-Lavega, S. Pérez-Hoyos, and R. Hueso, Am. J. Phys. **72**, 767 (2004).
[4] G. F. Lindal *et al.*, J. Geophys. Res. **92**, 14 987 (1987).
[5] M. G. Tomasko *et al.*, Nature (London) **438**, 765 (2005).
[6] M. Fulchignoni *et al.*, Nature (London) **438**, 785 (2005).
[7] R. Hueso and A. Sánchez-Lavega, Nature (London) **442**, 428 (2006).
[8] T. Tokano *et al.*, Nature (London) **442**, 432 (2006).
[9] S. K. Atreya *et al.*, Planet. Space Sci. **54**, 1177 (2006).
[10] J. H. Seinfeld and S. N. Pandis, *Atmospheric Chemistry and Physics* (Wiley, New York, 1998).
[11] K. C. Young, *Microphysical Processes in Clouds* (Oxford University Press, New York, 1993).
[12] B. J. Murray, D. A. Knopf, and A. K. Bertram, Nature (London) **434**, 202 (2005).
[13] J. P. Devlin, C. Joyce, and V. Buch, J. Phys. Chem. A **104**, 1974 (2000).
[14] M. Jetzki, A. Bonnamy, and R. Signorell, J. Chem. Phys. **120**, 11 775 (2004).
[15] S. Bauerecker, Phys. Rev. Lett. **94**, 033404 (2005).
[16] G. Firanescu, D. Hermsdorf, R. Ueberschaer, and R. Signorell, Phys. Chem. Chem. Phys. **8**, 4149 (2006).
[17] G. Firanescu, D. Luckhaus, and R. Signorell, J. Chem. Phys. **125**, 144501 (2006).
[18] C. Chapados and A. Cabana, Can. J. Chem. **50**, 3521 (1972).
[19] R. K. Khanna and M. Ngoh, Spectrochim. Acta, Part A **46**, 1057 (1990).
[20] W. Z. Alsindi, D. O. Gardner, E. F. van Dishoeck, and H. J. Fraser, Chem. Phys. Lett. **378**, 178 (2003).
[21] W. Press, J. Chem. Phys. **56**, 2597 (1972).
[22] M. Prager and W. Press, J. Chem. Phys. **92**, 5517 (1990).
[23] M. A. Neumann *et al.*, J. Chem. Phys. **119**, 1586 (2003).
[24] H. M. James and T. A. Keenan, J. Chem. Phys. **31**, 12 (1959).
[25] T. Yamamoto, Y. Kataoka, and K. Okada, J. Chem. Phys. **66**, 2701 (1977).
[26] K. Kobashi, K. Okada, and T. Yamamoto, J. Chem. Phys. **66**, 5568 (1977).
[27] D. M. Hudgins, S. A. Sandford, L. J. Allamandola, and A. G. G. M. Tielens, Astrophys. J. Suppl. Ser. **86**, 713 (1993).
[28] C. F. Bohren and D. R. Huffman, *Absorption and Scattering of Light by Small Particles* (Wiley-Interscience, New York, 1998).
[29] C. Gutt *et al.*, Phys. Rev. B **59**, 8607 (1999).